2013

Multi-species SIR models from a dynamical bayesian perspective

Lili Zhuang
Ohio State University

Noel Cressie
University of Wollongong, ncressie@uow.edu.au

Laura Pomeroy
Ohio State University

Daniel Janies
University of North Carolina at Charlotte

NIASRA

NATIONAL INSTITUTE FOR APPLIED STATISTICS RESEARCH AUSTRALIA

National Institute for Applied Statistics Research Australia

The University of Wollongong

Working Paper

05-13

Multi-species SIR Models from a Dynamical Bayesian Perspective

Lili Zhuang, Noel Cressie, Laura Pomeroy and Daniel Janies

National Institute for Applied Statistics Research Australia, University of Wollongong, Wollongong NSW 2522. Phone +61 2 4221 5435, Fax +61 2 4221 4845. Email: anica@uow.edu.au

Theoretical Ecology manuscript No.
(will be inserted by the editor)

Multi-species SIR Models from a Dynamical Bayesian Perspective

Lili Zhuang · Noel Cressie · Laura Pomeroy · Daniel Janies

Received: date / Accepted: date

Abstract Multi-species compartment epidemic models, such as the multi-species SIR (susceptible-infectious-recovered) model, are extensions of classic SIR models, used to explore the transient dynamics of pathogens that infect multiple hosts in a large population. In this article, we propose a dynamical Bayesian hierarchical SIR (HSIR) model, to capture the stochastic or random nature of an epidemic process in a multi-species SIR (with recovered becoming susceptible again) dynamical setting, under hidden mass-balance constraints. We call this an $\text{MSIR}_{\mathbf{B}}$ model. Different from a classic multi-species SIR model (which we call $\text{MSIR}_{\mathbf{C}}$), our approach imposes mass balance on the underlying

Corresponding Author
L. Zhuang
Department of Statistics
The Ohio State University
Columbus, OH 43210
Tel.: 614-292-2866
E-mail: zhuang.11@buckeyemail.osu.edu

N. Cressie
NIASRA
School of Mathematics and Applied Statistics
University of Wollongong
Wollongong, NSW 2522
Australia

L. Pomeroy
College of Veterinary Medicine
The Ohio State University
Columbus, OH 43210

D. Janies
Department of Bioinformatics and Genomics
University of North Carolina at Charlotte
Charlotte, NC 28223

true counts rather than, improperly, on the noisy observations. Moreover, the $\text{MSIR}_{\mathbf{B}}$ model can capture the discrete nature of, as well as uncertainties in, the epidemic process.

Keywords mass balance · epidemic model · influenza · HSIR · MSIR · disease dynamics

1 Introduction

1.1 Motivation

The influenza virus, a member of the *Orthomyxoviridae* family, infects multiple species worldwide, including poultry, swine, humans, horses, seals, and other animals (Webster et al, 1992; Alexander, 2000; Saenz et al, 2006; Munster et al, 2007; Nelson and Holmes, 2007; Stallknecht and Brown, 2007; Webby et al, 2007). Migratory waterfowl are the natural reservoir, maintaining the virus and occasionally infecting other hosts (Webster et al, 1992; Webby et al, 2007). Viral infection among humans and occasionally between animals and humans causes seasonal epidemics. In this viral-host system, it is important to understand between-species transmission for both veterinary health and human health.

Multi-species influenza transmission was observed in the 2009 H1N1 influenza pandemic, which was estimated to have caused 1.8 - 5.7 million human cases between April and July of 2009 in the United States alone (Reed et al, 2009). More recently, another multispecies strain, H3N2v, has emerged, but its burden has not yet been quantified (Nelson et al, 2012). Multi-species compartment epidemic models, such as the multi-species SIR (susceptible-infectious-recovered) model (e.g., Dobson, 2004), extend the traditional SIR model (Kermack and McKendrick, 1927) to explore the transient dynamics of pathogens that infect multiple host species. The model assumes that at any given time t, a fixed population can be split into three compartments (susceptible, infectious, and recovered); then in a multi-species SIR model, the dynamical process is captured through the following set of nonlinear ordinary differential equations (ODEs):

$$\frac{\mathrm{d}S_i}{\mathrm{d}t} = -\sum_{j=1}^{K} \beta_{ij} S_i I_j + \phi_i R_i, \tag{1}$$

$$\frac{\mathrm{d}I_i}{\mathrm{d}t} = \sum_{j=1}^{K} \beta_{ij} S_i I_j - \gamma_i I_i, \tag{2}$$

$$\frac{\mathrm{d}R_i}{\mathrm{d}t} = \gamma_i I_i - \phi_i R_i, \tag{3}$$

where i represents the i-th animal species, $i = 1, ..., K$, and K is the total number of species. We denote β_{ij} to be the transmission rate per unit time

from infectious individuals in the j-th species to susceptible individuals in the i-th species, which can be expressed as the fraction of contacts between the respective species that result in an infection. Hence, for $i = j$, β_{jj} is the within-species-j transmission rate per unit time, and for $i \neq j$, β_{ij} is the between-species transmission rate per unit time. Further, let γ_i denote the rate of "recovery" per unit time for species i, which is the rate at which infectious individuals are removed from being infectious due to recovery (or death); then $1/\gamma_i$ is the average infectious period. Let ϕ_i denote the rate of loss of immunity of recovered individuals per unit time for species i, which is the rate at which recovered individuals become susceptible again (Anderson and May, 1991; Hethcote, 2000; Arino et al, 2005); then $1/\phi_i$ is the average immunity period. At any given time t, $S_i(t)$, $I_i(t)$, and $R_i(t)$ are the numbers of susceptible, infectious, and recovered individuals of species i, $i = 1, ..., K$, respectively. Notice that (1)-(3) assume that there are no births or deaths from causes other than the disease itself; thus, the total number of susceptible, infectious, and recovered individuals of each species is assumed to be constant for a short period of time. Specifically, for any $t = 1, ..., T$,

$$S_i(t) + I_i(t) + R_i(t) = N_i, \tag{4}$$

where N_i is the size of the population of species i, $i = 1, ..., K$. This assumption is commonly referred to as *mass balance* (Reluga, 2004). Figure 1 shows the basic flow of individuals defined by this *classic multi-species SIR (*$\text{MSIR}_\mathbf{C}$*) model* in (1)-(3), which we call MSIRS flow; here, individuals of each species move from susceptible, to infectious, to recovered, and back to susceptible again. Individuals in the infectious state can infect not only susceptible individuals in the same species but also individuals from other species. It is a strength of the $\text{MSIR}_\mathbf{C}$ model (1)-(3), that if species i cannot be infected by species j (Scholtissek, 1990), then the cross-species infection rate β_{ij} is simply set equal to 0. Also notice that the $\text{MSIR}_\mathbf{C}$ model assumes a fraction of members of the recovered class can rejoin the susceptible class. Thus, it is also referred to as SIRS model in some articles (e.g., Arino, 2009); the traditional SIR model is obtained when $\phi_i = 0$, for $i = 1, ..., K$.

Similar to the classic SIR model, the $\text{MSIR}_\mathbf{C}$ model is appealing because of its straightforward modeling strategy and its easily interpretable parameters. However, as Zhuang (2011) pointed out (in a single species setting), there are various sources of uncertainty in the model. In our case, there may be uncertainty in the counts $\{S_i(t), I_i(t), R_i(t) : i = 1, ..., K\}$ themselves; that is, the counts in the compartments are observed with error. Another source of uncertainty in $\text{MSIR}_\mathbf{C}$, is that (1)-(3) may not capture the dynamics of the epidemic exactly. Moreover, the values of the parameters $\{\beta_{ij}\}$, $\{\gamma_i\}$, and $\{\phi_i\}$ are typically uncertain.

A variety of stochastic models with a probabilistic mechanism that involves a Markov chain of SIR states (also known as the master equation), have been developed recently (e.g., Ellner et al, 1998; Allen, 2003; Xu et al, 2007; Black and McKane, 2010; Jenkinson and Goutsias, 2012). However, these stochastic models ignore the noisy nature of data, and they improperly apply mass

balance to the *observed* counts. Furthermore, these models typically rely on many carefully chosen parameters, such as transmission rates, recovery rates, and so forth in heterogeneous populations; that is, uncertainty in where the parameter vector is located in the parameter space is not accounted for.

Bayesian hierarchical models have also proved popular for mapping non-infectious diseases; while these models aim to capture the true process hidden behind noisy data (e.g., Besag et al, 1991; Carlin and Banerjee, 2002), their process models and parameter models are not appropriate for epidemics. Those that do have a dynamical statistical component have not generally been parameterized in terms of the interpretable components of the epidemic (e.g., Mugglin et al, 2002; Wood, 2010). Further discussion is given in Zhuang (2011).

Recently, partially observed nonlinear stochastic dynamical systems (also know as partially observed Markov processes, or state-space models) have been used extensively for infectious-disease estimation and prediction. A wide range of inference techniques have been proposed and implemented in the R statistical language as part of the package pomp (http://cran.at.r-project.org/web/packages/pomp/), such as nonlinear forecasting (e.g., Kendall et al, 1999; Kendall et al, 2005), iterated filtering (Ionides et al, 2006; King et al, 2008; He et al, 2010), approximate Bayesian particle filtering (e.g., Liu and West, 2001; Arulampalam et al, 2001; Dukić et al, 2009). Some of these models are not appropriate for modeling epidemic flows (e.g., Kendall et al, 1999; Kendall et al, 2005). Those that are extensions of classic compartment epidemic models (e.g., SIR model and SEIR model), do pay attention to the underlying true process hidden behind the noisy data and incorporate a source of variation that captures randomness in the (hidden) epidemic process (e.g., Liu and West, 2001; Dukić et al, 2009). However, they do not preserve the mass-balance property when incorporating the extra source of variation, which may introduce biased results. Recent extensions to stochastic models with a master equation have similar problems with mass balance (e.g., Alonso et al, 2007).

In this article, we generalize the single-species approach of Zhuang (2011) to a multi-species setting, and we develop a mass-balanced discrete-time Bayesian hierarchical multi-species SIR ($\text{MSIR}_{\mathbf{B}}$) model, which allows us to capture the uncertainties in the underlying epidemic process without violating the mass-balance constraint on the true counts. Moreover, the $\text{MSIR}_{\mathbf{B}}$ model also retains the MSIRS flow defined in (1)-(3). Therefore, our approach can be used to study between-species transmission of disease and epidemics for both veterinary and human health.

In Section 2, we propose the $\text{MSIR}_{\mathbf{B}}$ model. For reasons of computational efficiency, a well calibrated linear approximation to the flow in the $\text{MSIR}_{\mathbf{B}}$ model is derived in Section 3. In Section 4, we discuss applications of our mathematical-statistical approach, and we simulate datasets to illustrate that its features are realistic. Section 5 gives a discussion and conclusions.

2 Bayesian Hierarchical Multi-species SIR ($\mathbf{MSIR_B}$) Model

We assume that underlying the observed epidemic counts, there is a true unobserved process, which we incorporate into the framework of a Bayesian hierarchical statistical model. This typically consists of three components: the data model (i.e., the conditional distribution of the data given hidden processes and parameters); the process model (i.e., the conditional distribution of the hidden processes given parameters); and the parameter model (i.e., the prior distribution of the parameters). This section generalizes the single-species Bayesian model proposed by Zhuang (2011).

2.1 Data Model

We model the raw counts directly rather than modeling the raw rates derived from the counts (e.g., Dukić et al, 2009, use Gaussian distributions to model the raw rates), and assume that the data model consists of (conditionally) independent Poisson distributions evolving at discrete time intervals. By including multiple host species, the data model in our case is

$$Z_S(t,i)|P_S(t,i) \sim \text{ind. Poisson}(\lambda_N(i)P_S(t,i)), \tag{5}$$

$$Z_I(t,i)|P_I(t,i) \sim \text{ind. Poisson}(\lambda_N(i)P_I(t,i)), \tag{6}$$

for time points $t = 1, 2, ..., T$, in units of Δ days, and species $i = 1, ..., K$. In (5) and (6), $Z_S(t,i)$ and $Z_I(t,i)$ are the observed number of susceptible and infectious individuals of species i at time t, respectively; "ind." is shorthand for "independent"; $\lambda_N(i)$ denotes the true total population count of species i, and $P_S(t,i)$ and $P_I(t,i)$ are the underlying true rates of susceptible and infectious individuals of species i at time t, respectively. We assume that $\lambda_N(i)$ is known for each species $i = 1, ..., K$, from demographic considerations, and $\{\lambda_N(i)\}$ is analogous to $\{N_i\}$ given by (4) for the $\text{MSIR}_\mathbf{C}$ model. By subtraction, we can easily obtain the observed number of recovered individuals, $Z_R(t,i) = \lambda_N(i) - Z_S(t,i) - Z_I(t,i)$. Thus, the data are $\{(Z_S(t,i), Z_I(t,i)) : t = 1, 2, ..., T,\ i = 1, ..., K\}$. Notice that the joint modeling of multiple host species adds a layer of generality that accounts for the between-species transmission.

2.2 Process Model

Recall the $\text{MSIR}_\mathbf{C}$ model defined by (1)-(3), where mass balance is assumed for the *observed* population. However, the appropriate place to impose mass balance is on the true (hidden) process. Thus, for time $t = 1, 2, ...,$ in the multi-species setting with species $i = 1, ..., K$, we have

$$\lambda_S(t,i) + \lambda_I(t,i) + \lambda_R(t,i) = \lambda_N(i), \tag{7}$$

where $\lambda_S(t,i)$, $\lambda_I(t,i)$, and $\lambda_R(t,i)$ are the underlying true (but hidden) counts of susceptible, infectious, and recovered individuals at time t, respectively. Now define the true (hidden) rates, $P_S(t,i)$, $P_I(t,i)$, and $P_R(t,i)$, via

$$\lambda_S(t,i) \equiv \lambda_N(i)P_S(t,i), \tag{8}$$

$$\lambda_I(t,i) \equiv \lambda_N(i)P_I(t,i), \tag{9}$$

$$\lambda_R(t,i) \equiv \lambda_N(i)P_R(t,i), \tag{10}$$

where $P_R(t,i)$ denotes the underlying true rate of recovered individuals of species i at time t. Then, by substituting (8)-(10) into (7), it is straightforward to see that the mass balance in (7) (imposed on each species $i = 1, ..., K$) can be rewritten as,

$$P_S(t,i) + P_I(t,i) + P_R(t,i) = 1, \tag{11}$$

for $t = 1, 2, ...,$ and $i = 1, ..., K$. From the mass-balance assumption in (11), $P_R(t,i)$ is obtained by subtraction: For $t = 1, 2, ...,$ and $i = 1, ..., K$,

$$P_R(t,i) = 1 - P_S(t,i) - P_I(t,i). \tag{12}$$

Recall the easily interpretable dynamics in the classic multi-species ODEs defined by (1)-(3), which enables individuals to move from the susceptible state to the infectious state, then to the recovered state (and some individuals may become susceptible again). We recognize that for this MSIRS flow, t is discrete (in units of Δ days) by deriving a set of deterministic difference equations on the hidden process, $\lambda_S(t,i)$, $\lambda_I(t,i)$, and $\lambda_R(t,i)$. That is, for $t = 1, 2, ...,$ and $i = 1, ..., K$, the process model becomes,

$$\lambda_S(t+1,i) = \lambda_S(t,i) - \sum_{j=1}^{K} \beta_{ij}\lambda_S(t,i)\lambda_I(t,j)\Delta + \phi_i\lambda_R(t,i)\Delta, \tag{13}$$

$$\lambda_I(t+1,i) = \lambda_I(t,i) + \sum_{j=1}^{K} \beta_{ij}\lambda_S(t,i)\lambda_I(t,j)\Delta - \gamma_i\lambda_I(t,i)\Delta, \tag{14}$$

$$\lambda_R(t+1,i) = \lambda_R(t,i) + \gamma_i\lambda_I(t,i)\Delta - \phi_i\lambda_R(t,i)\Delta, \tag{15}$$

where the MSIRS flow has been preserved, and the rate parameters β_{ij}, ϕ_i, and γ_i are in units of per day (d^{-1}).

According to the definition of $\lambda_S(t,i)$, $\lambda_I(t,i)$, and $\lambda_R(t,i)$ in (8)-(10), we can rewrite equations (13)-(15) in terms of the true proportions, $P_S(t,i)$, $P_I(t,i)$, and $P_R(t,i)$:

$$P_S(t+1,i) = P_S(t,i) - \sum_{j=1}^{K} \beta_{ij}\lambda_N(j)P_S(t,i)P_I(t,j)\Delta + \phi_i P_R(t,i)\Delta, \tag{16}$$

$$P_I(t+1,i) = P_I(t,i) + \sum_{j=1}^{K} \beta_{ij}\lambda_N(j)P_S(t,i)P_I(t,j)\Delta - \gamma_i P_I(t,i)\Delta, \tag{17}$$

$$P_R(t+1,i) = P_R(t,i) + \gamma_i P_I(t,i)\Delta - \phi_i P_R(t,i)\Delta. \tag{18}$$

Deterministic equations in classic epidemic models, which are similar to those in (16)-(18) but with given coefficients, are unable to capture the uncertainties in the hidden epidemic model. In our case, notice that as part of the process model, equations (16)-(18) are no longer deterministic, but become random-coefficient difference equations with coefficients having probability distribution defined in Section 2.3. Importantly, the random-coefficient difference equations are still mass-balanced.

To further model the complexity while still preserving the mass balance, we apply the logit transformation to the true rates, which changes the range from $(0,1)$ to $(-\infty,\infty)$. That is, for $t = 1,2,...,$ and $i = 1,...,K$, define

$$W_S(t,i) \equiv \log\left(\frac{P_S(t,i)}{P_R(t,i)}\right), \tag{19}$$

$$W_I(t,i) \equiv \log\left(\frac{P_I(t,i)}{P_R(t,i)}\right), \tag{20}$$

where $W_S(t,i)$ and $W_I(t,i)$ are the log odds ratios of susceptible-over-recovered populations and infectious-over-recovered populations, respectively, for species i at time t. On the odds-ratio scale (**W**-scale), we construct our process model in terms of $\mathbf{W}(t,i) \equiv (W_S(t,i), W_I(t,i))'$:

$$\mathbf{W}(t+1,i) = \boldsymbol{\mu}^W(t,i) + \boldsymbol{\xi}(t+1,i), \tag{21}$$

for discrete time $t = 1,2,...,$ in units of Δ days, and for species $i = 1,...,K$.

We now discuss each of the components of (21), in turn. The vector $\boldsymbol{\mu}^W(t,i) \equiv (\mu_S^W(t,i), \mu_I^W(t,i))'$ is the dynamical process that captures the temporal dependence. In Appendix A.1, we derive the nonlinear dynamical structure of $\boldsymbol{\mu}^W(t,i)$ using (16)-(20). This derivation retains the MSIRS flow on the hidden process; that is, for discrete time $t = 1,2,...,$ in units of Δ days, and for species $i = 1,...,K$,

$$\begin{aligned}\mu_S^W(t,i) = {} & W_S(t,i) \\ & + \log\left[1 + \frac{\phi_i\Delta}{\exp(W_S(t,i))} - \sum_{j=1}^{K} \frac{\beta_{ij}\lambda_N(j)\exp(W_I(t,j))\Delta}{1+\exp(W_S(t,j))+\exp(W_I(t,j))}\right] \\ & + \log\left[\frac{1}{1+\gamma_i\exp(W_I(t,i))\Delta - \phi_i\Delta}\right],\end{aligned} \tag{22}$$

$$\begin{aligned}\mu_I^W(t,i) = {} & W_I(t,i) \\ & + \log\left[1 - \gamma_i\Delta + \frac{\exp(W_S(t,i))}{\exp(W_I(t,i))}\sum_{j=1}^{K} \frac{\beta_{ij}\lambda_N(j)\exp(W_I(t,j))\Delta}{1+\exp(W_S(t,j))+\exp(W_I(t,j))}\right] \\ & + \log\left[\frac{1}{1+\gamma_i\exp(W_I(t,i))\Delta - \phi_i\Delta}\right],\end{aligned} \tag{23}$$

where recall that β_{ij} is the transmission rate per day from infectious individuals in the j-th species to susceptible individuals in the i-th species; γ_i and ϕ_i are the recovery rate per day and loss-of-immunity rate per day, respectively, for the i-th species.

We denote the vector, $\boldsymbol{\xi}(t,i) \equiv (\xi_S(t,i), \xi_I(t,i))'$, to be the small-scale variation that captures the uncertainties in the hidden epidemic process. For $t = 1, 2, ...,$ and $i = 1, ..., K$, we define

$$\boldsymbol{\xi}(t,i) \sim \text{MVN}(\mathbf{0}, \boldsymbol{\Sigma}_\xi(t,i)), \tag{24}$$

a multivariate normal (MVN) distribution with mean $\mathbf{0}$ and diagonal covariance matrix $\boldsymbol{\Sigma}_\xi(t,i) \equiv \text{diag}(\sigma^2_{\xi_S}(t,i), \sigma^2_{\xi_I}(t,i))$, and with nonnegative variance-components, $\sigma^2_{\xi_S}(t,i)$ and $\sigma^2_{\xi_I}(t,i)$. Notice that the diagonal covariance matrix for the log odds ratio implies non-zero covariances for the true (hidden) rates, $P_S(t,i)$, $P_I(t,i)$, and $P_R(t,i)$, which is in line with the dependence between species counts generated from a multinomial distribution.

The strategy of transforming from the hidden proportion scale (**P**-scale) to the hidden log-odds-ratio scale (**W**-scale) and making the small-scale variation additive on the **W**-scale rather than on the **P**-scale, is the key to retaining the mass-balance constraint while allowing flexible MSIRS flow to be handled. When there is only one species (i.e., $K = 1$), the $\text{MSIR}_\mathbf{B}$ model is equivalent to the HSIR model proposed by Zhuang (2011).

2.3 Parameter Model

To complete the Bayesian hierarchical statistical model, we now specify the joint prior distribution for the parameters, which includes the transmission rates per unit time $\{\beta_{ij}\}$ from infectious individuals of species j to susceptible individuals of species i, where $i, j = 1, ..., K$; the rates of recovery per day $\{\gamma_i\}$ where $i = 1, ..., K$; the loss-of-immunity rates per day $\{\phi_i\}$ where $i = 1, ..., K$; variance components $\{\sigma^2_{\xi_S}(t,i)\}$ and $\{\sigma^2_{\xi_I}(t,i)\}$ where $t = 1, 2, ...,$ and $i = 1, ..., K$. It is straightforward to see that all rate parameters are in $(0,1)$, and all variance-component parameters are in $[0, \infty)$.

Assuming statistical independence of parameters and using $[Y]$ as generic notation for the probability distribution of Y, we assume that the parameter model can be written as,

$$[\{\beta_{ij}\}, \{\gamma_i\}, \{\phi_i\}, \{\sigma^2_{\xi_S}(t,i)\}, \{\sigma^2_{\xi_I}(t,i)\}] = \left(\prod_{i=1}^{K}\prod_{j=1}^{K}[\beta_{ij}]\right) \cdot \left(\prod_{i=1}^{K}[\gamma_i][\phi_i]\right) \cdot \left(\prod_{i=1}^{K}\prod_{t=1}^{T}[\sigma^2_{\xi_S}(t,i)][\sigma^2_{\xi_I}(t,i)]\right), \tag{25}$$

where the prior distributions of individual parameters are specified as follows:

$$\beta_{ij} \sim \text{Uniform}(0,1), \ i, j = 1, ..., K$$

$$\gamma_i \sim \text{Uniform}(0,1),\ i = 1, ..., K$$

$$\phi_i \sim \text{Uniform}(0,1),\ i = 1, ..., K$$

$$\sigma^2_{\xi_S}(t,i) \sim \text{ Inverse Gamma } (a_{\xi_S}(t,i), b_{\xi_S}(t,i)),\ t = 1, ..., T,\ i = 1, ..., K.$$

$$\sigma^2_{\xi_I}(t,i) \sim \text{ Inverse Gamma } (a_{\xi_I}(t,i), b_{\xi_I}(t,i)),\ t = 1, ..., T,\ i = 1, ..., K.$$

Notice that the Uniform distributions on the rate parameters could easily be replaced by the very flexible Generalized Beta distributions on their supports. The Inverse-Gamma hyperparameters can be specified to give a fairly vague prior; for example, $a_{\xi_S}(t,i) = a_{\xi_I}(t,i) = 0.25$ and $b_{\xi_S}(t,i) = b_{\xi_I}(t,i) = 0.4$ for $t = 1, 2, ...,$ and $i = 1, ..., K$.

3 W-Scale Approximations for the MSIR$_\mathbf{B}$ Model

Here, we derive a calibrated linear approximation to the nonlinear **W**-scale process in the MSIR$_\mathbf{B}$ model. From Appendix A.2, for $t = 1, 2, ...,$ and $i = 1, ..., K$, equation (21) in the MSIR$_\mathbf{B}$ model can be approximated by

$$\mathbf{W}(t+1,i) = \boldsymbol{\mu}^{LW}(t,i) + \boldsymbol{\zeta}(t+1,i), \tag{26}$$

where recall that $\mathbf{W}(t,i) \equiv (W_S(t,i), W_I(t,i))'$ is the true log-odds-ratio vector. In (26), the vector $\boldsymbol{\mu}^{LW}(t,i) \equiv (\mu_S^{LW}(t,i), \mu_I^{LW}(t,i))'$ is a linear dynamical process derived through Taylor-series expansions that approximate the nonlinear stochastic process $\boldsymbol{\mu}^{W}(t,i)$ defined in (22)-(23). From Appendix A.2, for $t = 1, 2, ...,$ and $i = 1, ..., K$,

$$\begin{aligned}\mu_S^{LW}(t,i) = \ & J_0(t,i) + J_1(t,i)W_S(t,i) + J_2(t,i)W_I(t,i) \\ & + J_3(t,i)\sum_{j=1}^{K}\left[G_0(t,j) + G_1(t,j)W_S(t,j) + G_2(t,j)W_I(t,j)\right],\end{aligned} \tag{27}$$

$$\begin{aligned}\mu_I^{LW}(t,i) = \ & J_4(t,i) + J_5(t,i)W_S(t,i) + J_6(t,i)W_I(t,i) \\ & + J_7(t,i)\sum_{j=1}^{K}\left[G_0(t,j) + G_1(t,j)W_S(t,j) + G_2(t,j)W_I(t,j)\right],\end{aligned} \tag{28}$$

where

$$\begin{aligned}J_0(t,i) \equiv \ & \log\hat{A}_1(t,i) + \frac{1 + \phi_i e^{(\hat{A}_5(t,i))}(1 - \hat{A}_5(t,i))\Delta}{\hat{A}_1(t,i)} - \log\hat{A}_2(t,i) \\ & - \left(\frac{1 - \phi_i\Delta}{\hat{A}_2(t,i)}\right) - \frac{\gamma_i e^{\hat{A}_6(t,i)}\left(1 - \hat{A}_6(t,i)\right)\Delta}{\hat{A}_2(t,i)},\end{aligned} \tag{29}$$

$$J_1(t,i) \equiv 1 - \frac{\phi_i e^{\hat{A}_5(t,i)}\Delta}{\hat{A}_1(t,i)}, \tag{30}$$

$$J_2(t,i) \equiv -\frac{\gamma_i e^{\hat{A}_6(t,i)}\Delta}{\hat{A}_2(t,i)}, \tag{31}$$

$$J_3(t,i) \equiv -\frac{\Delta}{\hat{A}_1(t,i)}, \tag{32}$$

$$\begin{aligned} J_4(t,i) \equiv\ & \log(\hat{A}_3(t,i)) + \frac{1-\gamma_i\Delta}{\hat{A}_3(t,i)} - \log(\hat{A}_2(t,i)) \\ & - \left(\frac{1-\phi_i\Delta}{\hat{A}_2(t,i)}\right) - \frac{\gamma_i e^{\hat{A}_6(t,i)}\left(1-\hat{A}_6(t,i)\right)\Delta}{\hat{A}_2(t,i)}, \end{aligned} \tag{33}$$

$$\begin{aligned} J_5(t,i) \equiv & \sum_{j=1}^{K} \beta_{ij}\lambda_N(j)\left(1 - \frac{1}{1-\hat{A}_7(t,j)} + \frac{\hat{A}_7(t,j)+B_0(t,j)}{(1-\hat{A}_7(t,j))^2}\right) \\ & \cdot\frac{e^{\hat{A}_8(t,i)}\Delta}{\hat{A}_3(t,i)}, \end{aligned} \tag{34}$$

$$\begin{aligned} & J_6(t,i) \equiv \\ & -\left[\frac{\gamma_i e^{\hat{A}_6(t,i)}\Delta}{\hat{A}_2(t,i)} + \sum_{j=1}^{K}\beta_{ij}\lambda_N(j)\left(1 - \frac{1}{1-\hat{A}_7(t,j)} + \frac{\hat{A}_7(t,j)+B_0(t,j)}{(1-\hat{A}_7(t,j))^2}\right)\right] \\ & \cdot\frac{e^{\hat{A}_8(t,i)}\Delta}{\hat{A}_3(t,i)}, \end{aligned} \tag{35}$$

and

$$J_7(t,i) \equiv \frac{e^{\hat{A}_8(t,i)}(1-\hat{A}_8(t,i))\Delta}{\hat{A}_3(t,i)}. \tag{36}$$

Also, for species $j = 1, ..., K$,

$$G_0(t,j) = \beta_{ij}\lambda_N(j)\left(1 - \frac{1}{1-\hat{A}_7(t,j)} + \frac{B_0(t,j)+\hat{A}_7(t,j)}{\left(1-\hat{A}_7(t,j)\right)^2}\right), \tag{37}$$

$$G_1(t,j) = \frac{\beta_{ij}\lambda_N(j)B_1(t,j)\Delta}{\left(1-\hat{A}_7(t,j)\right)^2}, \tag{38}$$

$$G_2(t,j) = \frac{\beta_{ij}\lambda_N(j)B_2(t,j)\Delta}{\left(1-\hat{A}_7(t,j)\right)^2}, \tag{39}$$

$$B_0(t,j) \equiv e^{\hat{A}_4(t,j)}(1-\hat{A}_4(t,j))B^*(t,j), \tag{40}$$

$$B_1(t,j) \equiv \frac{e^{\left(\hat{A}_5(t,j)+\hat{A}_4(t,j)\right)}(1-\hat{A}_4(t,j))}{(1-\hat{A}_9(t,j))^2} - e^{\hat{A}_4(t,j)}B^*(t,j), \tag{41}$$

$$B_2(t,j) \equiv e^{\hat{A}_4(t,j)}B^*(t,j), \tag{42}$$

and

$$B^*(t,j) \equiv \frac{1}{1-\hat{A}_9(t,j)} + \frac{e^{\hat{A}_5(t,j)}(\hat{A}_5(t,j)-1)-\hat{A}_9(t,j)}{(1-\hat{A}_9(t,j))^2}. \tag{43}$$

The general idea behind (27) and (28) is to use $\hat{A}_l(t,i)$, $l = 1,...,9$, as an initialization of the Taylor-series expansion of the nonlinear process $\boldsymbol{\mu}^W(t,i)$ in (21). Formulas for $\{\hat{A}_l(t,i) : l = 1,...,9\}$ and the quantity $\{A_l(t,i) : l = 1,...,9\}$ that it approximates, are given in Table 1. Notice that empirical values obtained from the data $\{Z_S(t,i)\}$ and $\{Z_I(t,i)\}$ are used to obtain $\hat{A}_l(t,i)$ close to $A_l(t,i)$.

Also, β_{0ij}, γ_{0i}, and ϕ_{0i} in Table 1 are initial values of β_{ij}, γ_i, and ϕ_i, respectively, for species $i,j = 1,...,K$, which are used to enhance the Taylor-series expansions. In the single-species case, Zhuang (2011) uses values obtained from the classic SIR model. Similarly, in our case, initial values of these parameters can obtained from the $\text{MSIR}_\mathbf{C}$ model. Preliminary analyses for the single-species case shows that Bayesian inference is not sensitive to the initializations (even in forecasting), because the small-scale-variation terms in the linear process can absorb the higher-order terms in the Taylor-series expansions (e.g., Cressie and Wikle, 2011, Section 7.3.3).

Now we discuss the small-scale variation vector $\boldsymbol{\zeta}(t,i) \equiv (\zeta_S(t,i), \zeta_I(t,i))'$ in (26), which captures the uncertainties in the epidemic process as well as the higher-order terms in the Taylor-series expansions. For $t = 1,2,...,$ and $i = 1,...,K$, we assume that

$$\boldsymbol{\zeta}(t,i) \sim \text{MVN}(\mathbf{0}, \boldsymbol{\Sigma}_\zeta(t,i)), \tag{44}$$

where $\boldsymbol{\Sigma}_\zeta(t,i) \equiv \text{diag}\left(\sigma^2_{\zeta_S}(t,i), \sigma^2_{\zeta_I}(t,i)\right)$ is the covariance matrix of $\zeta(t,i)$, and $\sigma^2_{\zeta_S}(t,i)$ and $\sigma^2_{\zeta_I}(t,i)$ are nonnegative variance-component parameters. Typically, the components of $\boldsymbol{\Sigma}_\zeta(t,i)$ are larger than the respective components of $\boldsymbol{\Sigma}_\xi(t,i)$, because $\{\zeta(t,i)\}$ also captures the higher-order terms left after matching the linear approximation.

Like the data model, the parameter model is unchanged, except that the subscript ξ is replaced with the subscript ζ; see Section 2.3 for details. Therefore, the hierarchical model that consists of the data model defined in (5)-(6), the linear dynamical process model for $\{\mathbf{W}(t,i)\}$ defined in (26), and the parameter model defined in (25) with ξ replaced by ζ, approximates the $\text{MSIR}_\mathbf{B}$ model and, because of its computational simplicity, it can be used in MCMC-based posterior analysis.

4 Applications in Influenza Ecology

4.1 Joint Posterior Distribution

From Section 3, a well calibrated Gaussian linear process can be derived to approximate the nonlinear process on the $\mathbf{W}$-scale in the $\text{MSIR}_{\mathbf{B}}$ model, which henceforth defines our process model. These improves computational efficiency in posterior analysis and forecasting, although the posterior distribution is not available analytically due to a normalizing constant that cannot be obtained in closed form. The joint posterior distribution of all "unknowns" is proportional to a product of the data model, the process model, and the parameter model. Notice that $\{W_S(t,i)\}$ and $\{W_I(t,i)\}$ are transformations of $\{P_S(t,i)\}$ and $\{P_I(t,i)\}$. Combining equations (54)-(55) in Appendix A.1, the data model given by (5)-(6) can be rewritten: For $t = 1, ..., T$, and $i = 1, ..., K$,

$$Z_S(t,i)|\mathbf{W}(t,i) \sim \text{ ind. Poisson}\left(\frac{\lambda_N(i)\exp(W_S(t,i))}{1+\exp(W_S(t,i))+\exp(W_I(t,i))}\right),$$

$$Z_I(t,i)|\mathbf{W}(t,i) \sim \text{ ind. Poisson}\left(\frac{\lambda_N(i)\exp(W_I(t,i))}{1+\exp(W_S(t,i))+\exp(W_I(t,i))}\right).$$

Write $\mathbf{Z}(t,i) \equiv (Z_S(t,i), Z_I(t,i))'$; hence, the joint posterior distribution of all unknowns can be obtained as follows:

$$\begin{aligned}
&[\{\beta_{ij}\}, \{\gamma_i\}, \{\phi_i\}, \{\sigma^2_{\zeta_S}(t,i)\}, \{\sigma^2_{\zeta_I}(t,i)\},\\
&\quad \{\mathbf{W}(t,i)\}|\mathbf{Z}(1,i), ..., \mathbf{Z}(T,i) : i = 1, ..., K]\\
&\propto \prod_{t=1}^{T}\prod_{i=1}^{K}[Z_S(t,i)|\mathbf{W}(t,i)] \cdot \prod_{t=1}^{T}\prod_{i=1}^{K}[Z_I(t,i)|\mathbf{W}(t,i)]\\
&\quad \cdot \prod_{i=1}^{K}[\mathbf{W}(1,i)|\sigma^2_{\zeta_S}(1,i), \sigma^2_{\zeta_I}(1,i)]\\
&\cdot \prod_{t=2}^{T}\prod_{i=1}^{K}[\mathbf{W}(t,i)|\beta_{i1}, ..., \beta_{iK}, \gamma_i, \phi_i,\\
&\qquad \mathbf{W}(t-1,1), ..., \mathbf{W}(t,K), \sigma^2_{\zeta_S}(t,i), \sigma^2_{\zeta_I}(t,i)]\\
&\cdot \prod_{i=1}^{K}[\sigma^2_{\zeta_S}(t,i)] \prod_{i=1}^{K}[\sigma^2_{\zeta_I}(t,i)] \prod_{i=1}^{K}[\gamma_i] \prod_{i=1}^{K}[\phi_i] \prod_{i=1}^{K}\prod_{j=1}^{K}[\beta_{ij}],
\end{aligned} \tag{45}$$

where at $t = 1$, $\mathbf{W}(1,i) \equiv (W_S(1,i), W_I(1,i))'$ has distribution,

$$\mathbf{W}(1,i)|\sigma^2_{\zeta_S}(1,i), \sigma^2_{\zeta_I}(1,i) \sim \text{MVN}\left(\boldsymbol{\mu}_W(1,i), \boldsymbol{\Sigma}_\zeta(1,i)\right).$$

There is strong prior information on what happens at $t = 1$, which allows the hyperparameter $\boldsymbol{\mu}_W(1,i)$ to be specified. For example, in Section 4.2, we specify it as,

$$\boldsymbol{\mu}_W(1,i) = \left(\log\left(\frac{0.97}{0.01}\right), \log\left(\frac{0.02}{0.01}\right)\right)' = (4.57, 0.69)'.$$

Regarding parameter-model specification, Section 2 gives quite vague priors for all the parameters.

The posterior can be obtained through a Markov chain Monte Carlo (MCMC) algorithm with a Gibbs sampler that incorporates Metropolis-Hastings steps where necessary (e.g., Waller et al, 1997). This is given in full detail in the single-species setting by Zhuang(2011, Chapter 3, pg 61-90), where the MCMC was implemented on simulated data. Notice that this is not a particle-filtering approach in which new data are used to update current and past posteriors without having to re-run an MCMC. A disadvantage of the classic $\text{MSIR}_{\mathbf{C}}$ model is that it is unable to provide any uncertainty measures to accompany its deterministic modeling strategy. In contrast, one of the advantages of the $\text{MSIR}_{\mathbf{B}}$ model and our hierarchical approach is that we can obtain uncertainty measures for any unknown quantity of interest, based on the posterior distribution.

4.2 Multi-species Case Study

As a case study, we investigate the transmission of the influenza virus between $K = 2$ species: poultry ($i = 1$) and swine ($i = 2$). The interaction of these animals could spread influenza between species, given the lack of prohibitive species barriers (Kuiken et al, 2006).

For illustration purposes, we consider a farm where there are 100 poultry and 100 swine; that is, $\lambda_N(1) = \lambda_N(2) = 100$. At the start of the epidemic (time $t = 1$), most of the population is susceptible; for each species, say that there are two infected individuals and one recovered individual, so that we assume the mean $\boldsymbol{\mu}_W(t, i)$ of the log-odds-ratio vector $\mathbf{W}(t, i)$ at $t = 1$ is,

$$\boldsymbol{\mu}_W(1, i) = \left(\log\left(\frac{0.97}{0.01}\right),\ \log\left(\frac{0.02}{0.01}\right)\right)' = (4.57, 0.69)',\ \text{for } i = 1, 2.$$

Now consider the transmission rates. As discussed in Section 1, there are two types of transmissions for multi-host pathogens, that is, within-species transmission ($\{\beta_{ii} : i = 1, ..., K\}$) and between-species transmission ($\{\beta_{ij} : i \neq j = 1, ..., K\}$). According to Dobson (2004), although pathogen transmission is always impacted by various factors, such as host physiology, behavior, immunity, and ecology, we can assume that between-species transmission is a function of the mean within-species transmission rates modified by a constant scaling factor that varies between 0 and 1. That is, for $i \neq j = 1, ..., K$, we model

$$\beta_{ij} = c_{ij}\left(\frac{\beta_{ii} + \beta_{jj}}{2}\right), \tag{46}$$

where the parameter $c_{ij} \in [0, 1]$ is defined as *between-species transmission scaling*. Dobson (2004) points out that this approach is appealing because, through a single parameter c_{ij}, we can study how the relative magnitude of within-species versus between-species transmission can affect the system dynamics.

For illustration, we assume that $c_{ij} = c_{ji} = c \in [0,1]$, for $i \neq j = 1, ..., K$. Thus, from (46), we have $\beta_{ij} = \beta_{ji}$, namely, between-host transmission is symmetric. In the following analysis, we investigate five successively decreasing values of c, namely $c = 1, 0.75, 0.5, 0.25$, and 0. When $c = 1$, poultry and swine are fully mixing, and hence an animal is equally likely to contact a member of its own species as it is to contact a member of the other species. The successively decreasing values of c represent decreasing degrees of interaction between species and, when $c = 0$, species do not interact.

According to Bouma et al (2009), the within-poultry transmission rate for influenza given low doses of the virus is 0.8 per day; therefore, we assume $\beta_{11} = 0.8/\lambda_N(1) = 0.008$. Saenz et al (2006) report the influenza transmission rate within swine as approximately 0.3, so we assume $\beta_{22} = 0.3/\lambda_N(2) = 0.003$. The between-species transmission rates are obtained by substituting β_{11} and β_{22} into equation (46). According to Bouma et al (2009) and Saenz et al (2006), we know that the average infectious period for poultry lasts 2 days and for swine it lasts 7 days. Therefore, we assume a recovery rate of $\gamma_1 = 1/2$ for poultry and $\gamma_2 = 1/7$ for swine. Moreover, due to a number of factors, including a loss of immunity within the animal and changes in the virus due to evolution, immunity will wane over time in both swine and poultry. For swine, immunity will last for at least 42 days (Vincent et al, 2008). The rate at which immunity is lost in swine is the inverse of the period over which the swine are immune, so that $\phi_2 = 1/42$; we round down and assume $\phi_2 = 0.02$. For the purpose of illustration, we also assume that $\phi_1 = 0.02$.

We now turn to the components of variance. We assume that $\sigma^2_{\xi_S}(t,i) = \sigma^2_{\xi_S}(i)$ and $\sigma^2_{\xi_I}(t,i) = \sigma^2_{\xi_I}(i)$, for $t = 1, 2, ..., T$, and $i = 1, 2$. Recall that the *signal-to-noise ratio* (SNR) can be defined as

$$\text{SNR} \equiv \frac{\mu}{\sigma}, \tag{47}$$

where μ is the signal mean and σ is the standard deviation of the noise. We denote $\text{SNR}_{W_S}(t,i)$ and $\text{SNR}_{W_I}(t,i)$ to be the SNR for the log odds ratios $W_S(t,i)$ and $W_I(t,i)$, respectively, of the i-th species at time t. Then, from (47), for $t = 1, 2, ..., T$, and $i = 1, 2$, we have

$$\text{SNR}_{W_S}(t,i) \equiv \frac{\mu_{W_S}(t,i)}{\sigma_{\xi_S}(t,i)}, \tag{48}$$

$$\text{SNR}_{W_I}(t,i) \equiv \frac{\mu_{W_I}(t,i)}{\sigma_{\xi_I}(t,i)}. \tag{49}$$

If we assume that at time $t = 1$, $i = 1, 2$,

$$\text{SNR}_{W_S}(1,i) = 10,$$

$$\text{SNR}_{W_I}(1,i) = 10,$$

then from (48) and (49), and assuming temporal homogeneity of the variance components, we have for $t = 1, 2, ..., T$, and $i = 1, 2$,

$$\sigma^2_{\xi_S}(t,i) = \sigma^2_{\xi_S}(1,i) = (0.457)^2 = 0.21,$$

$$\sigma^2_{\xi_I}(t,i) = \sigma^2_{\xi_I}(1,i) = (0.069)^2 = 0.005.$$

We simulate daily data (i.e., $\Delta = 1$) for $T = 45$ days based on the assumptions and parameters given above. Specifically, for $t = 1$, $i = 1, 2$, we simulate

$$\mathbf{W}(1,i) \sim \text{MVN}\left(\boldsymbol{\mu}_W(1,i), \boldsymbol{\Sigma}_\xi(1,i)\right),$$

where recall that $\boldsymbol{\Sigma}_\xi(1,i) = \text{diag}(\sigma^2_{\xi_S}(1,i), \sigma^2_{\xi_I}(1,i))$. For $t = 2, ..., 45$, we simulate $\{\mathbf{W}(t,i)\}$ using (21) and then obtain $\{\mathbf{P}(t,i)\}$ using the transformations defined in (19) and (20). Finally, we generate observed counts of susceptible and infectious individuals, $\{Z_S(t,i)\}$ and $\{Z_I(t,i)\}$, from the Poisson distribution defined in (5) and (6), conditional on $\{\mathbf{P}(t,i)\}$. These counts, $\{Z_S(t,i)\}$ and $\{Z_I(t,i)\}$, represent the $\text{MSIR}_\mathbf{B}$ *dataset.*

In order to compare the result to the $\text{MSIR}_\mathbf{C}$ model, we *modify* it by embedding it into a hierarchical statistical model. That is, we put a data-model level above it: For $t = 1, 2, ...,$ and $i = 1, ..., K$, we assume that

$$Z_S(t,i)|P_S(t,i) \sim \text{ind. Poisson}(\lambda_N(i)P_S(t,i)),$$

$$Z_I(t,i)|P_I(t,i) \sim \text{ind. Poisson}(\lambda_N(i)P_I(t,i)).$$

The process model itself is made up of random-coefficient difference equations,

$$P_S(t+1,i) = P_S(t,i) - \sum_{j=1}^{K} \beta_{ij}\lambda_N(j)P_S(t,i)P_I(t,j)\Delta + \phi_i P_R(t,i)\Delta,$$

$$P_I(t+1,i) = P_I(t,i) + \sum_{j=1}^{K} \beta_{ij}\lambda_N(j)P_S(t,i)P_I(t,j)\Delta - \gamma_i P_I(t,i)\Delta,$$

$$P_R(t+1,i) = P_R(t,i) + \gamma_i P_I(t,i)\Delta - \phi_i P_R(t,i)\Delta.$$

We put a parameter-model level below it:

$$[\{\beta_{ij}\}, \gamma_i, \phi_i] = [\gamma_i][\phi_i]\prod_{j=1}^{K}[\beta_{ij}],$$

that captures the probability distribution of the coefficients.

We then simulate daily data for $T = 45$ days from the modified $\text{MSIR}_\mathbf{C}$ model and compare it to the $\text{MSIR}_\mathbf{B}$ model using the same parameters and procedures as given above. This results in counts, $\{Z_S(t,i)\}$ and $\{Z_I(t,i)\}$, which we call the Mod-$\text{MSIR}_\mathbf{C}$ *dataset.*

Figures 2 and 3 show the observed infectious counts $\{Z_I(t,i)\}$ (dots) and true underlying pattern $\{\lambda_I(t,i)\}$ (lines) simulated from the $\text{MSIR}_\mathbf{B}$ model and from the Mod-$\text{MSIR}_\mathbf{C}$ model, respectively, for both poultry (red) and swine (blue); the between-species transmission scaling $c = 1, 0.75, 0.5, 0.25, 0$, generates the five plots (a)-(e) in each figure.

Comparing Figure 2 and Figure 3, we can clearly see that the underlying true process of Figure 3 is smoother, as expected, since the $\text{MSIR}_\mathbf{C}$ model does not capture any uncertainty in the hidden epidemic process. By contrast,

Figure 2 suggests that the $\text{MSIR}_{\mathbf{B}}$ model not only has the ability to capture the uncertainties in the underlying epidemic process, but it also retains the interpretable epidemic pattern defined via the $\text{MSIR}_{\mathbf{C}}$ model. Recall that the key issue that allows us to successfully model the uncertainties while retaining mass balance in the $\text{MSIR}_{\mathbf{B}}$ model is a scale transformation from the $\boldsymbol{\lambda}$-scale (count) to the $\mathbf{W}$-scale (log odds ratio). Figure 2 illustrates that we do not lose interpretability when we perform this scale transformation.

Comparing the five plots within each of Figure 2 and Figure 3, we can see that when there is no interaction between species (i.e., $c = 0$), as shown in both Figures 2(e) and 3(e), the infectious population of swine reaches its peak much later than that of poultry, because poultry have a much higher within-species transmission rate as well as a higher recovery rate. However, as the between-species transmission scale c increases, we can clearly see that the infectious populations of both species can reach their peaks earlier and achieve a higher value. Notice that this phenomenon is even more obvious in swine than in poultry (the infectious population of swine reaches its peak at around day 30 when $c = 0$, but it changes to around day 10 when $c = 1$); from Figure 2, the change of the infectious-peak time is not as obvious for poultry when randomness is included in the process model. Furthermore, the time difference between the infectious peaks of different species decreases quickly as c increases from 0 to 1; that is, disease dynamics become synchronized across species. When $c = 1$, the respective infectious populations reach their peak at almost the same time; see Figures 2 (a) and 2 (b). This is in line with our expectations, because when $c = 1$, swine and poultry are fully mixing, so the between-species transmission has the same large effect on both species. These results also show that in a multi-species setting, the between-species transmission is very important and should not be ignored.

5 Discussion and Conclusions

Building models that include both data variability and process variability is important. Species may not act in isolation, and hence it is also important to build multi-species dynamical models. In this article, we incorporate both and develop a mass-balanced, discrete-time Bayesian hierarchical multi-species SIR ($\text{MSIR}_{\mathbf{B}}$) model, which models counts directly. The HSIR model proposed by Zhuang (2011) is a single-species version of the $\text{MSIR}_{\mathbf{B}}$ model. These models preserve mass balance on the (hidden) true counts rather than on the observed counts, they capture the stochastic and discrete nature of the epidemic process, and through a log-odds-ratio transformation they preserve the MSIRS flow that underlies the classic MSIR ($\text{MSIR}_{\mathbf{C}}$) model.

In our case study for influenza in poultry and swine, we simulated datasets from $\text{MSIR}_{\mathbf{B}}$ and a hierarchical version of the $\text{MSIR}_{\mathbf{C}}$ model, respectively. From the simulation results, we see the importance of incorporating between-species transmission into the modeling. Furthermore, we see the advantages of the $\text{MSIR}_{\mathbf{B}}$ model in accounting for uncertainties in the epidemic process while

retaining the easily interpretable MSIRS flow that underlies the $\text{MSIR}_{\mathbf{C}}$ model. The framework of this case study can be extended to other species (including humans) and other diseases. The important parameters in our model are $\{\beta_{ij}\}$, which allow us to handle heterogeneous populations within a species and zero or asymmetric cross-species transmission rates.

In ongoing research, we are investigating more complicated epidemic dynamics that incorporate birth, death, and emigration/immigration processes for appropriate time periods. Finally, incorporation of the spatial aspect into these hierarchical dynamical models could be handled through vector-valued processes, although the form of such models would require careful incorporation of the aforementioned emigration/immigration processes (Hooten and Wikle, 2010).

Acknowledgements We would like to express our appreciation to the referees and the editor for their constructive comments, which led to important improvements. Cressie's research was partially supported by the Naval Surface Warfare Center, Dahlgren Division, under grant no. N00178-10-Q-3903. We acknowledge that this material is based upon work supported by, or in part by, the US Army Research Laboratory and Office under grant number W911NF-05-1-0271.

Appendix

A.1

By adapting the Bayesian nonlinear dynamical approach of Zhuang (2011) to the multi-species setting, we give the derivation of the nonlinear dynamical structure of $\boldsymbol{\mu}^W(t,i)$ defined by (22) and (23) in Section 2.2.

Assume $P_R(t,i) > 0$, for time $t = 1, 2, ...,$ and species $i = 1, ..., K$. From the difference equations (16)-(18), we obtain

$$\frac{P_S(t+1,i)}{P_R(t+1,i)} = \frac{P_S(t,i) - P_S(t,i)\sum_{j=1}^{K}\beta_{ij}\lambda_N(j)P_I(t,j)\Delta + \phi_i P_R(t,i)\Delta}{P_R(t,i) + \gamma_i P_I(t,i)\Delta - \phi_i P_R(t,i)\Delta}, \tag{50}$$

$$\frac{P_I(t+1,i)}{P_R(t+1,i)} = \frac{P_I(t,i) + P_S(t,i)\sum_{j=1}^{K}\beta_{ij}\lambda_N(j)P_I(t,j)\Delta - \gamma_i P_I(t,i)\Delta}{P_R(t,i) + \gamma_i P_I(t,i)\Delta - \phi_i P_R(t,i)\Delta}. \tag{51}$$

Notice that equations (50) and (51) can be rewritten as

$$\frac{P_S(t+1,i)}{P_R(t+1,i)} = \frac{\frac{P_S(t,i)}{P_R(t,i)} - \frac{P_S(t,i)}{P_R(t,i)} \cdot \left(\sum_{j=1}^{K}\beta_{ij}\lambda_N(j)P_I(t,j)\right)\Delta + \phi_i\Delta}{1 + \gamma_i\frac{P_I(t,i)}{P_R(t,i)}\Delta - \phi_i\Delta}, \tag{52}$$

$$\frac{P_I(t+1,i)}{P_R(t+1,i)} = \frac{\frac{P_I(t,i)}{P_R(t,i)} + \frac{P_S(t,i)}{P_R(t,i)} \cdot \left(\sum_{j=1}^{K}\beta_{ij}\lambda_N(j)P_I(t,j)\right)\Delta - \frac{\gamma_i P_I(t,i)}{P_R(t,i)}\Delta}{1 + \gamma_i\frac{P_I(t,i)}{P_R(t,i)}\Delta - \phi_i\Delta}. \tag{53}$$

From (19) and (20),

$$P_S(t,i) = \frac{\exp(W_S(t,i))}{1 + \exp(W_S(t,i)) + \exp(W_I(t,i))}, \tag{54}$$

$$P_I(t,i) = \frac{\exp(W_I(t,i))}{1 + \exp(W_S(t,i)) + \exp(W_I(t,i))}. \tag{55}$$

Then, substituting (54) and (55) into (12), we obtain

$$P_R(t,i) = \frac{1}{1 + \exp(W_S(t,i)) + \exp(W_I(t,i))}. \tag{56}$$

Hence,

$$\frac{P_S(t,i)}{P_R(t,i)} = \exp(W_S(t,i)), \tag{57}$$

$$\frac{P_I(t,i)}{P_R(t,i)} = \exp(W_I(t,i)). \tag{58}$$

For $t = 1, 2, ...,$ and $i = 1, ..., K$, substitute (56)-(58) into equations (52) and (53) to obtain:

$$\begin{aligned}\exp(W_S(t+1,i)) = \; & \exp(W_S(t,i)) \\ & \cdot \left[1 + \frac{\phi_i \Delta}{\exp(W_S(t,i))} - \sum_{j=1}^{K} \frac{\beta_{ij} \lambda_N(j) \exp(W_I(t,j)) \Delta}{1 + \exp(W_S(t,j)) + \exp(W_I(t,j))}\right] \\ & \cdot \frac{1}{[1 + \gamma_i \exp(W_I(t,i)) \Delta - \phi_i \Delta]},\end{aligned} \tag{59}$$

$$\begin{aligned}\exp(W_I(t+1,i)) = \; & \exp(W_I(t,i)) \\ & \cdot \left[1 - \gamma_i \Delta + \frac{\exp(W_S(t,i))}{\exp(W_I(t,i))} \sum_{j=1}^{K} \frac{\beta_{ij} \lambda_N(j) \exp(W_I(t,j)) \Delta}{1 + \exp(W_S(t,j)) + \exp(W_I(t,j))}\right] \\ & \cdot \frac{1}{[1 + \gamma_i \exp(W_I(t,i)) \Delta - \phi_i \Delta]}.\end{aligned} \tag{60}$$

Taking logrithms on both sides of (59)-(60), for $t = 1, 2, ...,$ and $i = 1, ..., K$, we obtain,

$$\begin{aligned}W_S(t+1,i) = \; & W_S(t,i) \\ & + \log\left[1 + \frac{\phi_i \Delta}{\exp(W_S(t,i))} - \sum_{j=1}^{K} \frac{\beta_{ij} \lambda_N(j) \exp(W_I(t,j)) \Delta}{1 + \exp(W_S(t,j)) + \exp(W_I(t,j))}\right] \\ & + \log\left[\frac{1}{1 + \gamma_i \exp(W_I(t,i)) \Delta - \phi_i \Delta}\right],\end{aligned} \tag{61}$$

$$\begin{aligned}W_I(t+1,i) = \; & W_I(t,i) \\ & + \log\left[1 - \gamma_i \Delta + \frac{\exp(W_S(t,i))}{\exp(W_I(t,i))} \sum_{j=1}^{K} \frac{\beta_{ij} \lambda_N(j) \exp(W_I(t,j)) \Delta}{1 + \exp(W_S(t,j)) + \exp(W_I(t,j))}\right] \\ & + \log\left[\frac{1}{1 + \gamma_i \exp(W_I(t,i)) \Delta - \phi_i \Delta}\right].\end{aligned} \tag{62}$$

Then (61) and (62) are used to define $\boldsymbol{\mu}^W(t,i)$ in the nonlinear autoregressive structure given by (21), which captures the uncertainties in the hidden epidemic process.

A.2

By adapting the Bayesian nonlinear dynamical approach of Zhuang (2011), we give the derivation of a well calibrated linear process $\{\boldsymbol{\mu}^{LW}(t,i)\}$, as defined by (27) and (28), to approximate $\{\boldsymbol{\mu}^W(t,i)\}$ given by (22) and (23). Specifically, we show that for $t = 1, 2, ...,$ and $i = 1, ..., K$, $\{\hat{A}_l(t,i) : l = 1, ..., 9\}$ in Table 1 are initial values of the nonlinear components in equations (22) and (23).

Consider $\mu_S^W(t,i)$ given by (22) and use a second-order Taylor-series expansion. The second term on the right-hand side is:

$$\begin{aligned}
&\log\left(1+\frac{\phi_i\Delta}{e^{W_S(t,i)}}-\sum_{j=1}^{K}\frac{\beta_{ij}\lambda_N(j)e^{W_I(t,j)}\Delta}{1+e^{W_S(t,j)}+e^{W_I(t,j)}}\right)\\
&= \log(A_1(t,i))+\log\left[1+\left(\frac{1+\frac{\phi_i\Delta}{e^{W_S(t,i)}}-\sum_{j=1}^{K}\frac{\beta_{ij}\lambda_N(j)e^{W_I(t,j)}\Delta}{\left(1+e^{W_S(t,j)}+e^{W_I(t,j)}\right)}}{A_1(t,i)}-1\right)\right]\\
&\approx \log(\hat{A}_1(t,i))+\left(\frac{1+\frac{\phi_i\Delta}{e^{W_S(t,i)}}-\sum_{j=1}^{K}\frac{\beta_{ij}\lambda_N(j)e^{W_I(t,j)}\Delta}{\left(1+e^{W_S(t,j)}+e^{W_I(t,j)}\right)}}{\hat{A}_1(t,i)}-1\right)\\
&\quad-\frac{1}{2}\left(\frac{1+\frac{\phi_i\Delta}{e^{W_S(t,i)}}-\sum_{j=1}^{K}\frac{\beta_{ij}\lambda_N(j)e^{W_I(t,j)}\Delta}{\left(1+e^{W_S(t,j)}+e^{W_I(t,j)}\right)}}{\hat{A}_1(t,i)}-1\right)^2. \qquad (63)
\end{aligned}$$

Now the nonlinear term, $\frac{e^{W_I(t,j)}}{\left(1+e^{W_S(t,j)}+e^{W_I(t,j)}\right)}$, in (63) can be further expanded using a second-order Taylor series expansion: For $t=1,2,...,$ and $j=1,...,K$,

$$\begin{aligned}
&\frac{e^{W_I(t,j)}}{\left(1+e^{W_S(t,j)}+e^{W_I(t,j)}\right)}\\
&=1-\frac{1}{1-\left(-\frac{e^{W_I(t,j)}}{1+e^{W_S(t,j)}}\right)}\\
&\approx 1-\left[\frac{1}{1-\hat{A}_7(t,j)}+\frac{-\frac{e^{W_I(t,j)}}{1+e^{W_S(t,j)}}-\hat{A}_7(t,j)}{(1-\hat{A}_7(t,j))^2}+\frac{\left(-\frac{e^{W_I(t,j)}}{1+e^{W_S(t,j)}}-\hat{A}_7(t,j)\right)^2}{(1-\hat{A}_7(t,j))^3}\right].
\end{aligned} \qquad (64)$$

Then the remaining nonlinear component in (64), $\frac{e^{W_I(t,j)}}{1+e^{W_S(t,j)}}$, is expanded using a second-order Taylor-series expansion:

$$\begin{aligned}
&\frac{e^{W_I(t,j)}}{1+e^{W_S(t,j)}}\\
&=\left[e^{(W_I(t,j)-W_S(t,j))}\right]\cdot\left[\frac{1}{1-(-e^{-W_S(t,j)})}\right]\\
&\approx\left[e^{\hat{A}_4(t,j)}\left(1+(W_I(t,j)-W_S(t,j)-\hat{A}_4(t,j))+\frac{1}{2}(W_I(t,j)-W_S(t,j)-\hat{A}_4(t,j))^2\right)\right]\\
&\quad\cdot\left[\frac{1}{1-\hat{A}_9(t,j)}+\frac{\left(-e^{-W_S(t,j)}-\hat{A}_9(t,j)\right)}{\left(1-\hat{A}_9(t,j)\right)^2}+\frac{-e^{W_S(t,j)}-\hat{A}_9(t,j)}{\left(1-\hat{A}_9(t,j)\right)^3}\right],
\end{aligned} \qquad (65)$$

and

$$e^{-W_S(t,j)} \approx e^{\hat{A}_5(t,j)} + e^{\hat{A}_5(t,j)}\left(-W_S(t,j) - \hat{A}_5(t,j)\right) + \frac{e^{\hat{A}_5(t,j)}\left(-W_S(t,j) - \hat{A}_5(t,j)\right)^2}{2}. \quad (66)$$

Upon substituting (66) into (65), we obtain:

$$\frac{e^{W_I(t,j)}}{1+e^{W_S(t,j)}} \approx B_0(t,j) + B_1(t,j)W_S(t,j) + B_2(t,j)W_I(t,j) + o(W_S(t,j)^2) + o(W_I(t,j)^2) + o\left(W_S(t,j)W_I(t,j)\right), \quad (67)$$

where $\{B_l(t,j) : l = 0,1,2\}$ are defined in equations (40)-(43).

Finally, combining (63), (64), and (67), we approximate the expression,

$$\log\left(1 + \frac{\phi_i \Delta}{e^{W_S(t,i)}} - \sum_{j=1}^{K} \frac{\beta_{ij}\lambda_N(j)e^{W_I(t,j)}\Delta}{1+e^{W_S(t,j)}+e^{W_I(t,j)}}\right),$$

in equation (22) with

$$\begin{aligned}
&\log\hat{A}_1(t,i) + \frac{1}{\hat{A}_1(t,i)} + \frac{\phi_i e^{(\hat{A}_5(t,i))}(1-\hat{A}_5(t,i))\Delta}{\hat{A}_1(t,i)} - 1 - \frac{\phi_i \exp(\hat{A}_5(t,i))}{\hat{A}_1(t,i)} W_S(t,i)\Delta \\
&- \frac{1}{A_1(t,i)} \sum_{j=1}^{K} \left[\beta_{ij}\lambda_N(j)\left(1 - \frac{1}{1-\hat{A}_7(t,j)} + \frac{B_0(t,j)+\hat{A}_7(t,j)}{(1-\hat{A}_7(t,j))^2}\right)\right. \\
&\quad \left. + \frac{\beta_{ij}\lambda_N(j)B_1(t,j)}{(1-\hat{A}_7(t,j))^2} W_S(t,j) + \frac{\beta_{ij}\lambda_N(j)B_2(t,j)}{(1-\hat{A}_7(t,j))^2} W_I(t,j)\right]\Delta \\
&+ \sum_{j=1}^{K}\left[o\left(W_S^2(t,j)\right) + o\left(W_I^2(t,j)\right) + o\left(W_S(t,j)W_I(t,j)\right)\right]. \quad (68)
\end{aligned}$$

Furthermore, the third term, $\log\left(1+\gamma_i e^{W_I(t,i)}\Delta - \phi_i\Delta\right)$, on the right-hand side of (22), can also be expanded in a second-order Taylor series expansion: For $t = 1,2,...,$ and $i = 1,...,K$,

$$\begin{aligned}
\log\left(1+\gamma_i e^{W_I(t,i)}\Delta - \phi_i\Delta\right) &= \log(A_2(t,i)) + \log\left[1 + \left(\frac{1+\gamma_i e^{W_I(t,i)}\Delta - \phi_i\Delta}{A_2(t,i)} - 1\right)\right] \\
&\approx \log(\hat{A}_2(t,i)) + \left(\frac{1+\gamma_i e^{W_I(t,i)}\Delta - \phi_i\Delta}{\hat{A}_2(t,i)} - 1\right) \\
&\quad - \frac{1}{2}\left(\frac{1+\gamma_i e^{W_I(t,i)}\Delta - \phi_i\Delta}{\hat{A}_2(t,i)} - 1\right)^2.
\end{aligned} \quad (69)$$

Also, to second order:

$$e^{W_I(t,i)} \approx e^{\hat{A}_6(t,i)} + e^{\hat{A}_6(t,i)}(W_I(t,i) - \hat{A}_6(t,i)) + \frac{e^{\hat{A}_6(t,i)}}{2}(W_I(t,i) - \hat{A}_6(t,i))^2. \quad (70)$$

Upon substituting (70) into (69), we obtain:

$$\log\left(1+\gamma_i e^{W_I(t,i)}\Delta-\phi_i\Delta\right) \approx \log\hat{A}_2(t,i)+\frac{1}{\hat{A}_2(t,i)}+\frac{\gamma_i}{\hat{A}_2(t,i)}e^{\hat{A}_6(t,i)} \cdot(1-\hat{A}_6(t,i))\Delta-\frac{\phi_i\Delta}{\hat{A}_2(t,i)}-1 +\frac{\gamma_i e^{\hat{A}_6(t,i)}}{\hat{A}_2(t,i)}W_I(t,i)\Delta+o\left(W_I^2(t,i)\right). \quad (71)$$

Consider $\mu_I^W(t,i)$ given by (23) and use a second-order Taylor-series expansion; the second term on the right-hand side is:

$$\begin{aligned}
&\log\left(1-\gamma_i\Delta+\frac{\exp\left(W_S(t,i)\right)}{\exp\left(W_I(t,i)\right)}\sum_{j=1}^{K}\frac{\beta_{ij}\lambda_N(j)e^{W_I(t,j)}\Delta}{1+e^{W_S(t,j)}+e^{W_I(t,j)}}\right)\\
&= \log(A_3(t,i))+\log\left[1+\left(\frac{1-\gamma_i\Delta+\frac{\exp(W_S(t,i))}{\exp(W_I(t,i))}\sum_{j=1}^{K}\frac{\beta_{ij}\lambda_N(j)e^{W_I(t,j)}\Delta}{1+e^{W_S(t,j)}+e^{W_I(t,j)}}}{A_3(t,i)}-1\right)\right]\\
&\approx \log(\hat{A}_3(t,i))+\left(\frac{1-\gamma_i\Delta+\frac{\exp(W_S(t,i))}{\exp(W_I(t,i))}\sum_{j=1}^{K}\frac{\beta_{ij}\lambda_N(j)e^{W_I(t,j)}\Delta}{1+e^{W_S(t,j)}+e^{W_I(t,j)}}}{\hat{A}_3(t,i)}-1\right)\\
&\quad-\frac{1}{2}\left(\frac{1-\gamma_i\Delta+\frac{\exp(W_S(t,i))}{\exp(W_I(t,i))}\sum_{j=1}^{K}\frac{\beta_{ij}\lambda_N(j)e^{W_I(t,j)}\Delta}{1+e^{W_S(t,j)}+e^{W_I(t,j)}}}{\hat{A}_3(t,i)}-1\right)^2. \qquad (72)
\end{aligned}$$

Recall that the approximation to the nonlinear term, $\frac{e^{W_I(t,j)}}{\left(1+e^{W_S(t,j)}+e^{W_I(t,j)}\right)}$, in (72) can be obtained through (64). Now, $\frac{\exp(W_S(t,i))}{\exp(W_I(t,i))}$ can be further expanded using a second-order Taylor-series expansion:

$$\begin{aligned}
\frac{e^{(W_S(t,i))}}{e^{(W_I(t,i))}} &= e^{W_S(t,i)-W_I(t,i)}\\
&\approx e^{\hat{A}_8(t,i)}+e^{\hat{A}_8(t,i)}\left(W_S(t,i)-W_I(t,i)-\hat{A}_8(t,i)\right)\\
&\quad+\frac{e^{\hat{A}_8(t,i)}}{2}\left(W_S(t,i)-W_I(t,i)-\hat{A}_8(t,i)\right)^2. \qquad (73)
\end{aligned}$$

Finally, combining (64), (72), and (73), we approximate the expression,

$$\log\left[1-\gamma_i\Delta+\frac{\exp\left(W_S(t,i)\right)}{\exp\left(W_I(t,i)\right)}\sum_{j=1}^{K}\frac{\beta_{ij}\lambda_N(j)e^{W_I(t,j)}\Delta}{1+e^{W_S(t,j)}+e^{W_I(t,j)}}\right],$$

in equation (23) with

$$\log\hat{A}_3(t,i)+\frac{1-\gamma_i\Delta}{\hat{A}_3(t,i)}-1$$

$$+\left[\sum_{j=1}^{K}\beta_{ij}\lambda_N(j)\left(1-\frac{1}{1-\hat{A}_7(t,j)}+\frac{\hat{A}_7(t,j)+B_0(t,j)}{\left(1-\hat{A}_7(t,j)\right)^2}\right)\Delta\right]\frac{e^{\hat{A}_8(t,i)}W_S(t,i)}{\hat{A}_3(t,i)}$$

$$-\left[\sum_{j=1}^{K}\beta_{ij}\lambda_N(j)\left(1-\frac{1}{1-\hat{A}_7(t,j)}+\frac{\hat{A}_7(t,j)+B_0(t,j)}{\left(1-\hat{A}_7(t,j)\right)^2}\right)\Delta\right]\frac{e^{\hat{A}_8(t,i)}W_I(t,i)}{\hat{A}_3(t,i)}$$

$$+\frac{e^{\hat{A}_8(t,i)}\left(1-\hat{A}_8(t,i)\right)\Delta}{\hat{A}_3(t,i)}\cdot\sum_{j=1}^{K}\left[\beta_{ij}\lambda_N(j)\right.$$

$$\left.\cdot\left(1-\frac{1}{1-\hat{A}_7(t,j)}+\frac{\hat{A}_7(t,j)+B_0(t,j)}{\left(1-\hat{A}_7(t,j)\right)^2}+\frac{B_1(t,j)W_S(t,j)}{\left(1-\hat{A}_7(t,j)\right)^2}+\frac{B_2(t,j)W_I(t,j)}{\left(1-\hat{A}_7(t,j)\right)^2}\right)\right]$$

$$+\sum_{j=1}^{K}\left[o\left(W_S(t,j)^2\right)+o\left(W_I(t,j)^2\right)+o\left(W_S(t,j)W_I(t,j)\right)\right]. \tag{74}$$

Finally, the third component on the right-hand side of (23) is identical to that of (22).

Therefore, (68), (71), and (74) yield the linear dynamical process $\boldsymbol{\mu}^{LW}(t,i)$ as defined in (27) and (28) in Section 3. That is, $\boldsymbol{\mu}^{LW}(t,i)$ approximates the nonlinear dynamical process, $\boldsymbol{\mu}^{W}(t,i)$, in the $\text{MSIR}_{\mathbf{B}}$ model defined by equations (22) and (23).

References

Alexander DJ (2000) A review of avian influenza in different bird species. Veterinary Microbiology 74:3–13

Allen L (2003) An Introduction to Stochastic Processes with Applications to Biology. Prentice-Hall, Upper Saddle River, NJ.

Alonso D, McKane AJ, Pascual M (2007) Stochastic amplification in epidemics. Journal of the Royal Society Interface 4(14):575–582

Anderson R, May R (1991) Infectious Diseases of Humans: Dynamics and Control. Oxford University Press, Oxford

Arino J (2009) Diseases in metapopulations. In: Ma Z, Zhou Y, Wu J (eds) Series in Contemporary Applied Mathematics., World Scientific, Singapore., vol 11, pp 65–123

Arino J, Davis J, Hartley D, Jordan R, Miller J, Van Den Driessche P (2005) A multi-species epidemic model with spatial dynamics. Mathematical Medicine and Biology 22:129–142

Arulampalam S, Maskell S, Gordon N, Clapp T (2001) A tutorial on particle filters for on-line non-linear/non-Gaussian Bayesian tracking. IEEE Transactions on Signal Processing 50:174–188

Besag J, York J, Mollié A (1991) Bayesian image restoration, with two applications in spatial statistics. Annals of the Institute of Statistical Mathematics 43:1–59

Black AJ, McKane AJ (2010) Stochasticity in staged models of epidemics: quantifying the dynamics of whooping cough. Journal of the Royal Society Interface 7:1219–1227

Bouma A, Claassen I, Natih K, Klinkenberg D, Donnelly C, Koch G, van Boven M (2009) Estimation of transmission parameters of H5N1 avian influenza virus in chickens. PLOS Pathogens 5(1):e1000,281

Carlin B, Banerjee S (2002) Hierarchical multivariate CAR models for spatio-temporally correlated survival data (with discussion). In: Bernardo J, Bayarri M, Berger J, Dawid A, Heckerman D, Smith AFM, West M (eds) in Bayesian Statistics 7, Clarendon Press, Oxford., pp 45–63

Cressie N, Wikle C (2011) Statistics for Spatio-Temporal Data. Wiley, Hoboken, NJ.

Dobson A (2004) Population dynamics of pathogens with multiple host species. The American Naturalist 164:S64–S78

Dukić V, Lopes HF, Polson NG (2009) Tracking flu epidemics using Google trends and particle learning. Working paper, University of Chicago Booth School of Business, *Chicago, IL*

Ellner SP, Bailey BA, Bobashev GV, Gallant AR, Grenfell BT, Nychka DW (1998) Noise and nonlinearity in measles epidemics: combining mechanistic and statistical approaches to population modeling. The American Naturalist 151(5):425–440

He D, Ionides EL, King AA (2010) Plug-and-play inference for disease dynamics: measles in large and small populations as a case study. Journal of the Royal Society Interface 7:271–283

Hethcote HW (2000) The mathematics of infectious diseases. SIAM Review 42:599–653

Hooten MB, Wikle CK (2010) Statistical agent-based models for discrete spatio-temporal systems. Journal of the American Statistical Association 105:236–248

Ionides EL, Bretó C, King AA (2006) Inference for nonlinear dynamical systems. Proceedings of the National Academy of Sciences of the United States of America 103:18,438–18,443

Jenkinson G, Goutsias J (2012) Numerical integration of the master equation in some models of stochastic epidemiology. PLoS ONE 7:e36,160

Kendall BE, Briggs CJ, Murdoch WW, Turchin P, Ellner SP, McCauley E, Nisbet RM, Wood SN (1999) Why do populations cycle? a synthesis of statistical and mechanistic modeling approaches. Ecology 80:1789–1805

Kendall BE, Ellner SP, McCauley E, Wood SN, Briggs CJ, Murdoch WM, Turchin P (2005) Population cycles in the pine looper moth: dynamical tests of mechanistic hypotheses. Ecological Monographs 75:259–276

Kermack W, McKendrick A (1927) Contributions to the mathematical theory of epidemics - I. Proceedings of the Royal Society of Edinburgh A 115:700–721

King AA, Ionides EL, Pascual M, Bouma MJ (2008) Inapparent infections and cholera dynamics. Nature 454:877–880

Kuiken T, Holmes E, McCauley J, Rimmelzwaan G, Williams C, Grenfell B (2006) Host species barriers to influenza virus infections. Science 312:394–397

Liu J, West M (2001) Combined parameter and state estimation in simulation-based filtering. In: Doucet A, de Freitas N, Gordon NJ (eds) Sequential Monte Carlo Methods in Practice, Springer, New York, pp 197–224

Mugglin A, Cressie N, Gemmell I (2002) Hierarchical statistical modelling of influenza epidemic dynamics in space and time. Statistics in Medicine 21:2703–2721

Munster V, Baas C, Lexmond P, Waldenström J, Wallensten A, Fransson T, Rimmelzwaan GF, Beyer WEP, Schutten M, Olsen B, Osterhaus ADME, Fouchier RAM (2007) Spatial, temporal, and species variation in prevalence of influenza A viruses in wild migratory birds. PLoS Pathogens 3:e61

Nelson MI, Holmes EC (2007) The evolution of epidemic influenza. Nature Reviews Genetics 8:196–205

Nelson MI, Vincent AL, Kitikoon P, Holmes EC, Gramer MR (2012) Evolution of novel reassortant A/H3N2 influenza viruses in north American swine and humans, 2009-2011. Journal of Virology 86(16):8872–8878

Reed C, Angulo FJ, Swerdlow DL, Lipsitch M, Meltzer MI, Jernigan D, Finelli L (2009) Estimates of the prevalence of pandemic H1N1 2009, United States, April-July 2009. Emerging Infectious Diseases 15:2004–2007

Reluga T (2004) A two-phase epidemic driven by diffusion. Journal of Theoretical Biology 229:249–261

Saenz RA, Hethcote HW, Gray GC (2006) Confined animal feeding operations as amplifiers of influenza. Vector-Borne and Zoonotic Diseases 6:338–346

Scholtissek C (1990) Pigs as 'mixing vessels' for the creation of new pandemic influenza A viruses. Medical Principles and Practice 2:65–71

Stallknecht DE, Brown JD (2007) Wild birds and the epidemiology of avian influenza. Journal of Wildlife Diseases 43:S15–S20

Vincent A, Ma W, Lager K, Janke B, Richt J (2008) Swine influenza viruses: A North American perspective. Advances in Virus Research 72:127–154

Waller L, Carlin B, Xia H, Gelfand A (1997) Hierarchical spatio-temporal mapping of disease rates. Journal of the American Statistical Association 92:607–617

Webby RJ, Webster RG, Richt JA (2007) Influenza viruses in animal wildlife populations. Current Topics in Microbiology and Immunology 315:67–83

Webster RG, Bean WJ, Gorman OT, Chambers TM, Kawaoka Y (1992) Evolution and ecology of influenza A viruses. Microbiology and Molecular Biology Reviews 56:152–179

Wood SN (2010) Statistical inference for noisy nonlinear ecological dynamic systems. Nature 466:1102–1104

Xu Y, Allena L, Perelson A (2007) Stochastic model of an influenza epidemic with drug resistance. Journal of Theoretical Biology 248:179–193

Zhuang L (2011) Bayesian Dynamical Modeling of Count Data. PhD Thesis. Department of Statistics, The Ohio State University, http://etd.ohiolink.edu/view.cgi/Zhuang%20Lili.pdf?osu1315949027

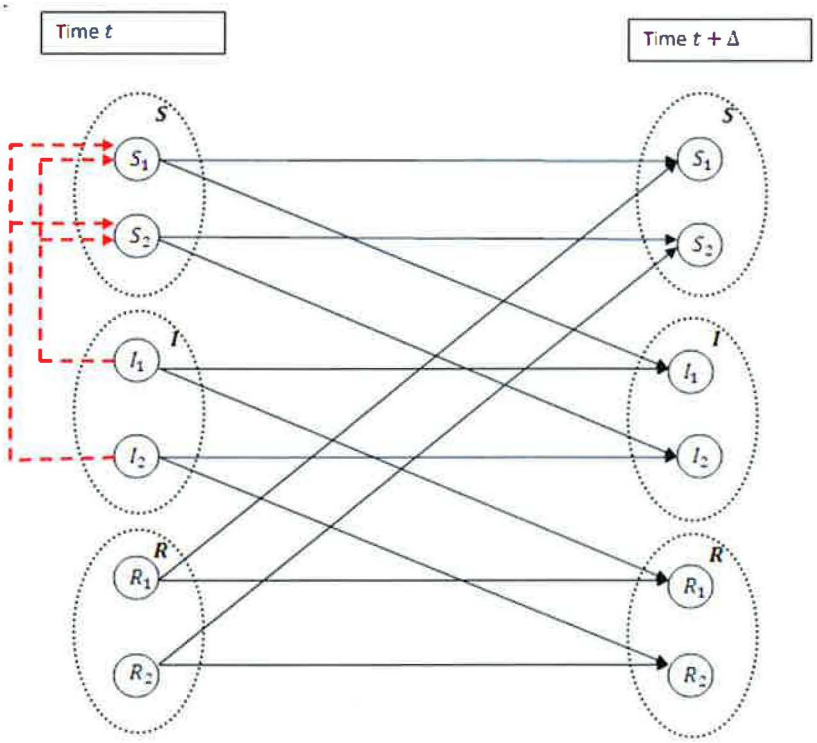

Fig. 1 A basic MSIRS flow defined by a classic multi-species SIR ($\text{MSIR}_{\mathbf{C}}$) model from time t to $t+\Delta$. Black arrows indicate disease progression through time, as a susceptible individual becomes infected and then has the possibility to recover. Red dashed arrows indicate a latent virus-feedback procedure (transmission from infectious individuals to susceptible individuals).

Table 1 Table of the initializations $\{\hat{A}_l(t,i) : l = 1,...,9\}$ and the quantities $\{A_l(t,i) : l = 1,...,9\}$ that they approximate

Value	Initializations ($\hat{A}_l(t,i)$)	Nonlinear Components in MSIR_{B} ($A_l(t,i)$)
$A_1(t,i)$	$1+\frac{\phi_{0i}Z_R(t,i)\Delta}{Z_S(t,i)}-\sum_{j=1}^{K}\beta_{0ij}Z_I(t,j)\Delta$	$1+\frac{\phi_i}{e^{W_S(t,i)}}-\sum_{j=1}^{K}\frac{\beta_{ij}\lambda_N(j)e^{W_I(t,j)}}{1+e^{W_S(t,j)}+e^{W_I(t,j)}}\Delta$
$A_2(t,i)$	$1+\gamma_{0i}\frac{Z_I(t,i)}{Z_R(t,i)}\Delta-\phi_{0i}\Delta$	$1+\gamma_i e^{W_I(t,i)}\Delta-\phi_i\Delta$
$A_3(t,i)$	$1-\gamma_{0i}\Delta+\frac{Z_S(t,i)}{Z_I(t,i)}\sum_{j=1}^{K}\beta_{0ij}Z_I(t,j)\Delta$	$1-\gamma_i\Delta+\frac{e^{W_S(t,i)}}{e^{W_I(t,i)}}\sum_{j=1}^{K}\frac{\beta_{ij}\lambda_N(j)e^{W_I(t,j)}\Delta}{1+e^{W_S(t,j)}+e^{W_I(t,j)}}$
$A_4(t,i)$	$\log\frac{Z_I(t,i)}{Z_R(t,i)}-\log\frac{Z_S(t,i)}{Z_R(t,i)}$	$W_I(t,i)-W_S(t,i)$
$A_5(t,i)$	$-\log\frac{Z_S(t,i)}{Z_R(t,i)}$	$-W_S(t,i)$
$A_6(t,i)$	$\log\frac{Z_I(t,i)}{Z_R(t,i)}$	$W_I(t,i)$
$A_7(t,i)$	$-\frac{Z_I(t,i)}{(\lambda_N(i)-Z_I(t,i))}$	$-\frac{e^{(W_I(t,i))}}{(1+e^{(W_S(t,i))})}$
$A_8(t,i)$	$-\log\frac{Z_I(t,i)}{Z_R(t,i)}+\log\frac{Z_S(t,i)}{Z_R(t,i)}$	$-W_I(t,i)+W_S(t,i)$
$A_9(t,i)$	$-\frac{Z_R(t,i)}{Z_S(t,i)}$	$-e^{-W_S(t,i)}$

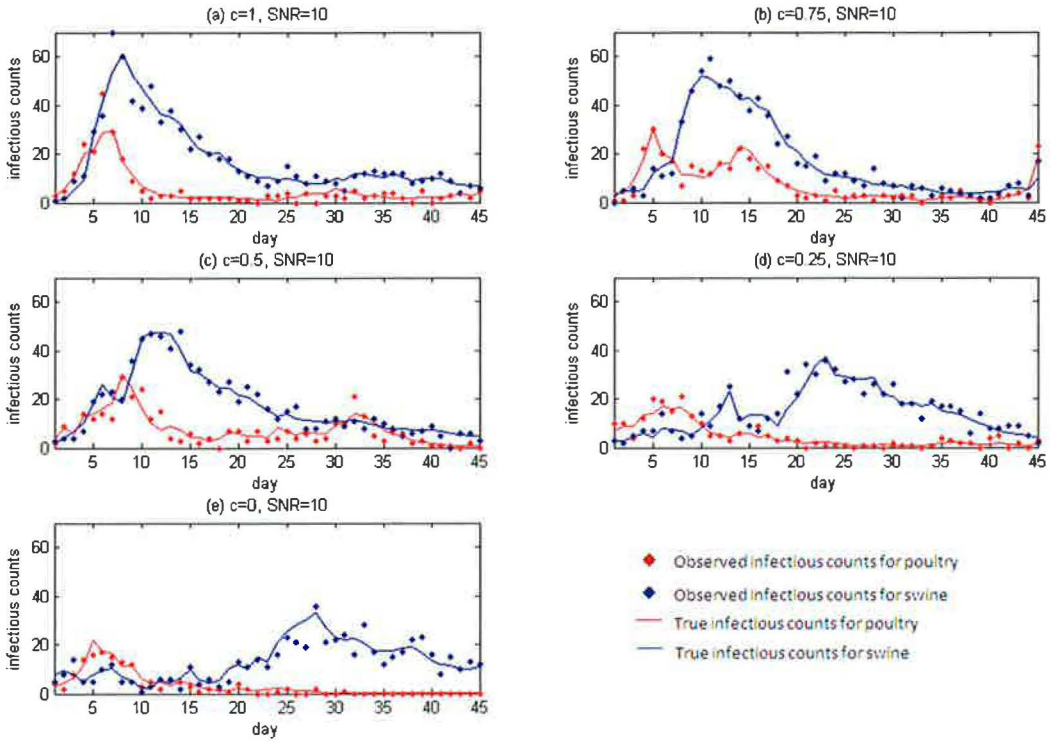

Fig. 2 Plots of observed infectious counts $\{Z_I(t,i)\}$ (dots) and true infectious counts $\{\lambda_I(t,i)\}$ (lines) simulated from the MSIR_B model for poultry (red) and swine (blue), respectively. Figures (a)-(e) correspond to $c = 1, 0.75, 0.5, 0.25, 0$, respectively.

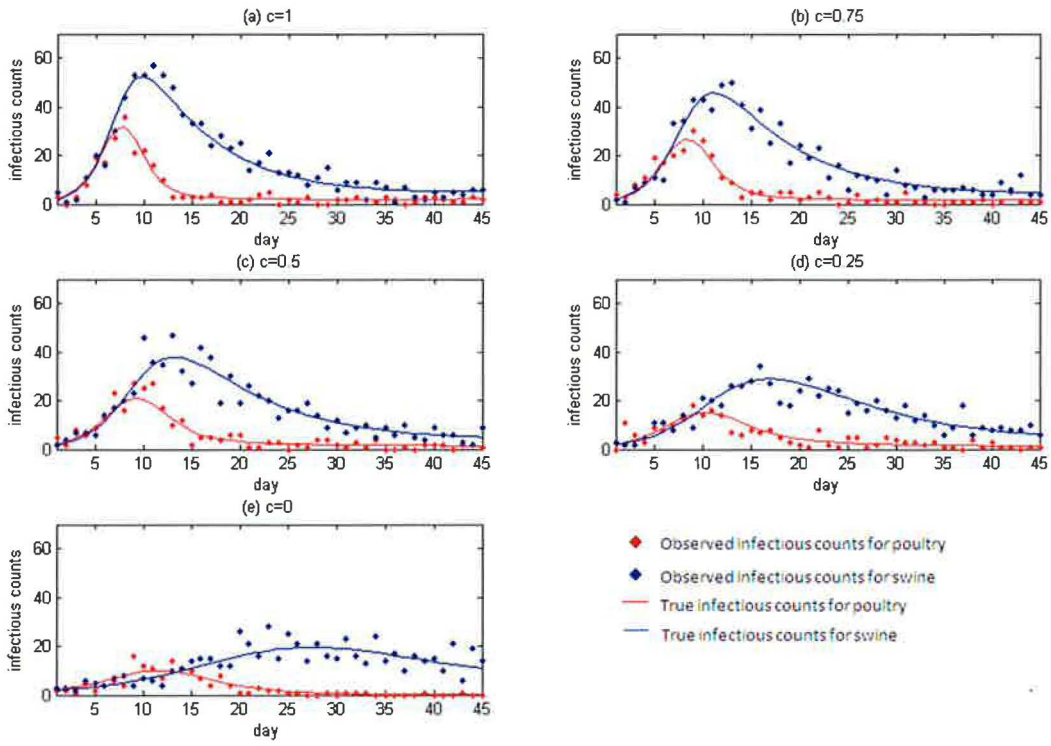

Fig. 3 Plots of observed infectious counts $\{Z_I(t,i)\}$ (dots) and true infectious counts $\{\lambda_I(t,i)\}$ (lines) simulated from the Mod-MSIR$_{\mathbf{C}}$ model for poultry (red) and swine (blue), respectively. Figures (a)-(e) correspond to $c = 1, 0.75, 0.5, 0.25, 0$, respectively.